A New Metric for Latent Fingerprint Image Preprocessing

Haiying Guan, Andrew M. Dienstfrey, and Mary Frances Theofanos
National Institute of Standards and Technology, USA
{haiying.guan, andrew.dienstfrey, and mary.theofanos}@nist.gov

Abstract

We propose a new image-based metric and explore its utility as a quality diagnostic for fingerprint image preprocessing. Due to the low quality of the latent fingerprint images, preprocessing is a common step in the forensic analysis workflow, and furthermore is critical to the success of fingerprint identification. Whereas fingerprint analysis is a well-studied field with a deep history, forensic image preprocessing is a relatively new domain in need of research and development of analysis and best practice guidance.

Our new metric is based on an extension of the Spectral Image Validation and Verification (SIVV) [1]. SIVV was originally developed to differentiate ten-print or rolled fingerprint images from other non-fingerprint images such as face or iris images. Several modifications are required to extend SIVV analysis to the latent space. We propose, implement, and test this new SIVV-based metric to measure latent fingerprint image quality and the effectiveness of the forensic latent fingerprint preprocessing step. Preliminary results show that this new metric can provide positive indications of both latent fingerprint image quality, and the effectiveness of fingerprint preprocessing.[1]

1. Introduction

The performance of a fingerprint recognition system is heavily dependent on the quality of the collected fingerprint images. This poses a problem for latent fingerprints as their image quality is generally low due to the combination of difficulties in lifting the print from substrate, and image contamination by complex background noise. As a result, fingerprint structures such as minutiae and ridges may not be clearly visible to the human eye of a fingerprint examiner, nor to the computational eye of automatic matching systems.

Due to the poor quality of latent fingerprint images, digital image preprocessing is generally a necessary step in the forensic analysis workflow [2] [2]. Image preprocessing is performed to increase latent fingerprint image quality. Some of the common transformations employed in service of this goal include: color management, contrast adjustment, edge enhancement, background suppression, and noise filtration.

The necessity and prevalence of latent fingerprint image preprocessing belies the fact that it is not a single activity but rather a complex process containing several sub-varieties. For one, different image software systems use different implementations of even the most basic image functions. See, for example, the multiple implementations of RGB-to-grey-scale conversation. Even more, the same fingerprint may be enhanced in different ways as fingerprint examiners may have their own analysis style. Finally, the desired endpoints of an enhancement may be different and matching systems can have distinct criteria for their input. The overarching principle for image preprocessing is that the image transformations should neither add to, nor subtract from, fingerprint information contained within image. This guiding principle presently lacks analytical underpinnings.

Although latent fingerprints are well and widely studied by forensic scientists [3], there has been little systematic analysis of the latent fingerprint image preprocessing. Latent fingerprint preprocessing is a relatively new area requiring research in order to be put on firmer foundations. It is especially critical to perform research of the fingerprint preprocessing image transformations, and to propose effective approaches or give general suggestions to guide the preprocessing workflow. Our objective is to research and develop metrics that characterizes the image processing performed in the course of forensic analysis of latent fingerprint images to serve as a bridge between theory and practice.

The research community has developed several approaches and algorithms for fingerprint image quality [4] [5] and latent fingerprint enhancement [6]. Yoon, *et al.* [6] proposed a latent fingerprint enhancement algorithm requiring a manually marked region of interest (ROI) and singular points. The paper proposed a novel orientation field estimation algorithm, which fits the coarse orientation map to an orientation field model. Experimental results on the NIST SD27 Latent Fingerprint Database [7] indicate that, with the use of the proposed enhancement algorithm, the matching accuracy of the commercial matcher was improved.

[1] This work is an official contribution of the National Institute of Standards and Technology and not subject to copyright in the United States.

[2] This was formerly referred to as "image enhancement," however the new term of art is "image preprocessing", which is language used herein.

In this paper, we focus attention on the preprocessing step absent mark-up of orientation fields and minutiae. We seek to compare the image qualities of *before images* — original RGB images, directly obtained from forensic crime scene photography—and *after images*—the grey-scale image after preprocessing—to evaluate the performance of the preprocessing procedure.[3]

We base our new metric on an extension of the Spectral Image Verification and Validation analysis (SIVV) [1] to the forensic latent fingerprint preprocessing domain. The original SIVV algorithm was designed for image validation and verification of ten-print fingerprint images from live-scan devices, and for maintaining the fidelity of fingerprint image databases. SIVV can effectively differentiate the non-fingerprint input from the flat or rolled fingerprint input[4]. As the periodic structure of the fingerprint ridges and furrows is a level one feature, SIVV is potentially applicable to the latent fingerprint preprocessing domain. However, latent fingerprints are largely corrupted by complex background noise and the ridge structures are not clearly visible. Furthermore, latent images are of poor quality and the fingerprints can be incomplete. In summary, the SIVV feature analysis as originally developed cannot be directly applied to the latent fingerprint images.

We implemented several modifications to adapt SIVV to latent fingerprints to resolve the above-mentioned difficulties. In order to suppress confounding background noise, the following refinements are proposed: in the spatial domain, the algorithm focuses on the region of interest of a fingerprint; in the frequency domain, the algorithm constrains the SIVV peak to be within a limited range, which can be inferred by the fingerprint ridges' pixel distances on the latent fingerprint images. The resulting metric is still based on the intrinsic Fourier spectral properties of latent fingerprint images. The new latent fingerprint quality metric provides the quantitative measurement to characterize the quality of the latent fingerprint images and measures the effectiveness of the latent fingerprint preprocessing process.

2. Fingerprint quality measurement metric

The objective of most digital preprocessing technology applied to latent fingerprint images is to show more contrast between ridges and furrows, allowing for clearer identification of minutia points. The ridges and furrows appear as periodic structures in the fingerprint image. This periodicity manifests as spikes in the frequency spectrum of the image. Such a signal (spike) in the frequency domain is a good metric to measure the image quality of the ridges and furrows. Thus, we are going to measure the latent fingerprint quality based on it.

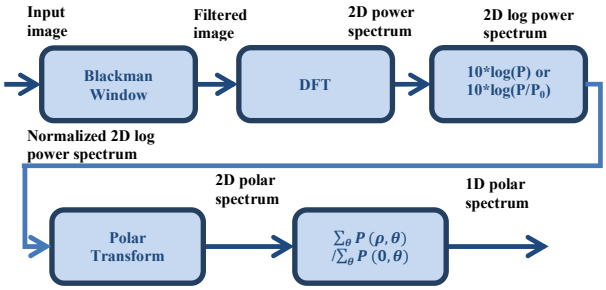

Figure 1: SIVV algorithm.

2.1. SIVV on flat/ten-print or rolled fingerprint

SIVV analysis derives from the periodicity of ridges and furrows [1]. For completeness, first we summarize the SIVV algorithm (for the detailed presentation, please refer to the original report [1]). The algorithm proceeds as follows:

Step 1. Image Windowing

One dimensional Blackman window is given in the following equation:

$$w(n) = 0.42 - 0.5\cos\left(\frac{2\pi n}{N-1}\right) + 0.08\cos\left(\frac{4\pi n}{N-1}\right) \quad (1)$$
$$where\ 0 \le n \le N-1$$

The length of the one dimensional window is N. Given the image with N rows and M columns, the two dimensional Blackman Window is the tensor product of windows of length N and M. When the 2D Blackman Window is applied to the fingerprint image, the window is applied on the center of the fingerprint texture and the size is adapted to the size of the fingerprint image.

Step 2. Discrete Fourier Transform (DFT)

$$H(u,v) = \sum_{x=0}^{M-1}\sum_{y=0}^{N-1} \exp\left[2\pi i y\frac{v}{N}\right]\exp\left[2\pi i x\frac{u}{M}\right]h(x,y) \quad (2)$$

Here u and v denote frequency components in the x and y directions ranging from $\frac{-M}{2}$ to $\frac{M}{2}$ and $\frac{-N}{2}$ to $\frac{N}{2}$ respectively.

Step 3. 2D (normalized) Log Power Spectrum

The 2D power spectrum is computed as:

$$P(u,v) = |H(u,v)|^2 \quad (3)$$

[3] Note, we are not aware of a database of fingerprint images suitable for the present analysis. The latent fingerprint images shown here were obtained in collaboration with Mathew Schwarz of Schwarz Forensics and David "Ski" Witzke of Foray Technologies. A more extensive, public available collection of images would be invaluable for future work in this area.

[4] The experiment shows 10% equal error rate (EER, which is where false accept rate and false reject rate are the same,) for differentiating the fingerprints mixed with a variety of non-fingerprint images in [1]'s application domain.

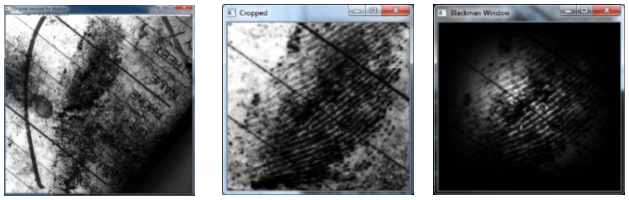

(a) Original image (b) Cropped image (c) After Blackman window

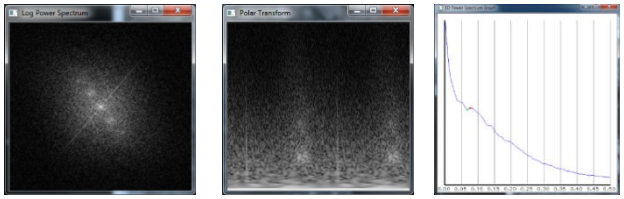

(d) 2D power spectrum (e) 2D log polar spectrum (f) 1D log polar spectrum

Figure 2: An example of the SIVV feature on a latent fingerprint image (courtesy of SIVV software package in NBIS [8]), the original image is G001L2U.tif, ROI: [206 97 514 417]).

Depending on the implementation, the output of this step can be normalized or not-normalized; that is

$$10 * logP(u,v) \tag{4}$$

Or

$$10 * log\frac{P(u,v)}{P(0,0)} \tag{5}$$

Step 4. 2D Polar Transform of Power Spectrum

The 2D power spectrum is represented in polar coordinates using the transformation:

$$\rho = \frac{\sqrt{u^2+v^2}}{\sqrt{M^2+N^2}} \tag{6}$$

$$\theta = tan^{-1}\left(\frac{v}{u}\right) \tag{7}$$

We use $P(\rho,\theta)$ to represent the 2D results of the polar transformation, where ρ is divided by the maximum dimension of the input image N, normalized to 0 and 0.5 cycles/pixels.

Step 5. 1D Normalized Polar Transform

Finally, the 1D polar transform is computed as the sum over angles of:

$$P(\rho) = \sum_{\theta=0}^{180} P(\rho,\theta) \tag{8}$$

$$\rho = 0,\dots,0.5 \quad cycles/pixels$$

The normalized 1D polar curve is:

$$P_N(\rho) = \frac{P(\rho)}{P(0)} \tag{9}$$

$$\rho = 0,\dots,0.5 \quad cycles/pixels$$

The algorithm schematic is shown in Figure 1.

2.2. Motivation of our approach

The original SIVV feature performs well on flat/ten-prints or rolled fingerprints, which are captured by inking methods or live scan devices in an attended mode. In such contexts, background noise is minimized during the capture, and the contrast between the ridges and furrows is relatively high. As image quality is generally controlled very well, the fingerprint image ridges and valleys are clear and computer readable. In such cases, the periodic structure of the ridges and valleys can be captured by Fourier spectrum analysis in the frequency domain. It follow that SIVV performs well when a fingerprint image is of good quality.

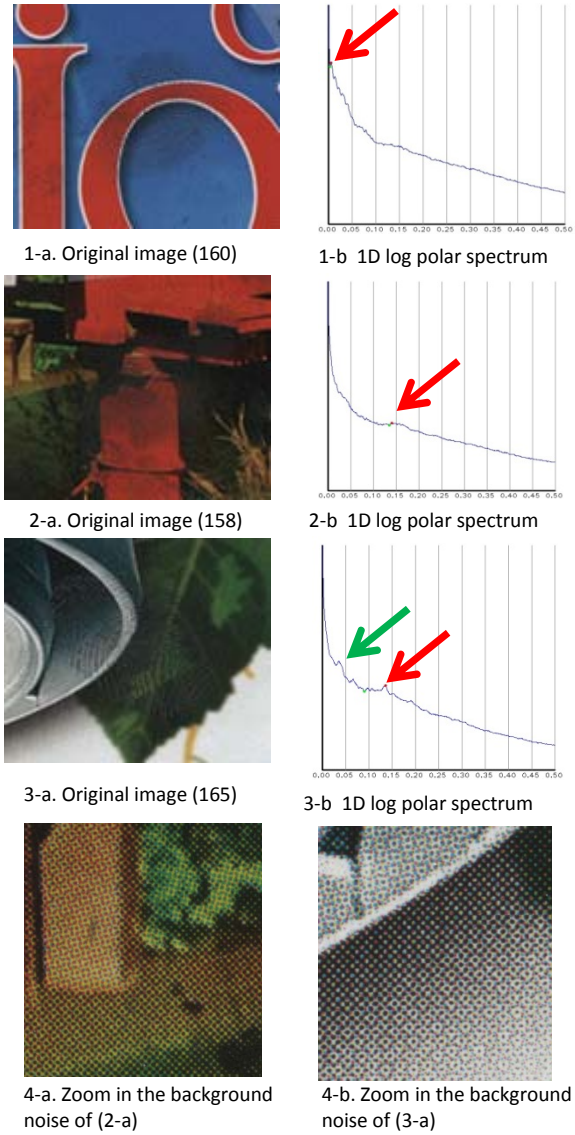

1-a. Original image (160) 1-b 1D log polar spectrum

2-a. Original image (158) 2-b 1D log polar spectrum

3-a. Original image (165) 3-b 1D log polar spectrum

4-a. Zoom in the background noise of (2-a) 4-b. Zoom in the background noise of (3-a)

Figure 3: Examples of the SIVV feature on a latent fingerprint image (courtesy of [8]: the implementation convert RGB image to gray-level image before applying the core SIVV algorithm. We show RGB images for better illustration purpose, and we also want to differentiate before (RGB) from after (gray-level) images.).

However, latent fingerprints are generally smudgy and blurred. They often capture only a small finger area, and may have large nonlinear distortion due to pressure variations. And there may be terrible unavoidable background noise which is extremely hard to model because of the large variety of background colors, textures etc. When background noise is strong, the fingerprint ridges and furrows' peak spike is easily mixed up or embedded by the signals of other periodic structures of the images, such as with the textile fabric, or any other patterned noises.

Figure 2 shows an example of original SIVV (implementation courtesy of [8]) on a latent fingerprint image in the NIST Database 27 [8]. It shows that the SIVV spike is largely weakened due to the fingerprint incompleteness and from being submerged in the background noise.

Figure 3 shows the examples of original SIVV results (implementation provided by [8]) on the latent fingerprint images in our forensic latent fingerprint preprocessing dataset. It shows that the original SIVV implementation cannot be directly applied on latent fingerprint images. In the first case, 1-a, 1-b, and 2-a, 2-b, there is no obvious spike at all. In the third case, 3-a, 3-b, the detected peak (red arrow) actually does not represent the fingerprint ridges and furrows; it represents the texture of the background, which is shown in 4-a and 4-b (the detailed tiny grids on the images). The actual fingerprint ridge peak is shown by the green arrow in 3-b.

Given a poor quality image with partial fingerprint or large background noise, the SIVV spike is weakened and submerged into the background noise. Generally, SIVV cannot be directly applied to the latent fingerprints in most cases. In this paper, in order to identify, enhance, and recover the SIVV spike, we proposed two approaches: Region of Interest (ROI) to focus only on the local region which contains fingerprint signal in spatial domain; and the peak location constraint to focus on the small window which may contain the ridge and furrow spike in the frequency domain.

2.3. Blackman window

The objective of the Blackman window is to suppress the noise outside of the fingerprint region. Due to the latent fingerprint's location, orientation, and shape (partial fingerprint prints) changes, we add more flexibility in application of the Blackman window filter to the image. First, we can control the shape of the Blackman Window using more general equations:

$$w(n) = \frac{1-\alpha}{2} - \frac{1}{2}\cos\left(\frac{2\pi n}{N-1}\right) + \frac{\alpha}{2}\cos\left(\frac{4\pi n}{N-1}\right) \quad (10)$$

$$\boldsymbol{where\ 0 \le n \le N-1}$$

α is a variable which decides the shape of the Blackman bell. The unqualified term *Blackman window* in the previous equation Eq. (1) refers to α = 0.16 (red curve in Figure 4). Figure 4 shows the shape given different α values. When α increases, the bell shape becomes narrow, and the boundary signal in images is suppressed; when α is decreased, the bell is wider, and the boundary signal in the image widow is included; when α is negative, the bell becomes even wider. We suggest utilizing a monotonous curve (from the center of the curve to the boundary of the window). The green and dark purple curves in Figure 4 are not recommended (the values are not monotonous and decrease from the center to the tails of the curve).

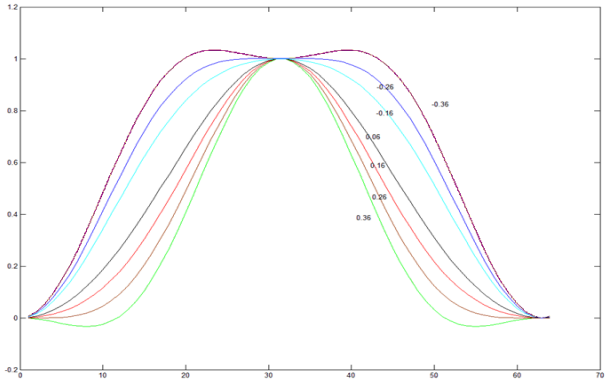

Figure 4: General Blackman Window given different α value.

We also include additional parameters to control the location and orientation of the Blackman window. In practice, if the fingerprint boundary contains large noise, we may choose a narrow shape to reduce the noise effect: if the fingerprint boundary is clear, we may choose a wide shape to increase more ridge furrow patterns and to increase the SIVV feature strength. Figure 5 contrasts the following SIVV results: no Blackman window (Figure 5-a), original Blackman window (Figure 5-b) and a customized Blackman window (Figure 5-c). It shows that the regular Blackman window does help to strengthen the fingerprint signal in some cases. The customized Blackman Window has more flexibility to select the best region, which is very useful to latent fingerprint image analysis because the location, orientation, and portion of the print vary greatly in latent fingerprints.

2.4. Region of Interests (ROI)

Fingerprint images often include the background noise where the image was collected. The noise can be classified into two types: the noise in the area inside the actual fingerprint region, and the noise in the area outside the actual fingerprint region. It is very difficult to remove the noise in the area inside the actual fingerprint region. However, it is relatively easy to remove the background noise in the area outside of the actual fingerprint region and is important to do so because this region does not provide usable information but may contribute a large amount of noise that will submerge the fingerprint SIVV

feature in the frequency domain. We first remove it from the spatial domain before we calculate the FFT features in the frequency domain.

Because SIVV is not invariant to translation and is sensitive to noise, the spectral analysis must be focused on a region of interest (ROI) with significant fingerprint patterns; that is, the image region which contains the most fingerprint information. Figure 5-d shows the comparison of SIVV curves using the whole image and the ROI. The SIVV spike (indicated with arrow) of the ROI image is much stronger than the SIVV spike of the whole image. The example shows that focusing on the ROI helps to recover the SIVV feature from the noise background.

The signal strength of the SIVV peak is mainly related to two factors. One is the frequency power of the finger print ridge and furrow, which is related to the area size of the fingerprint region; that is the larger area includes more ridges and furrows and thus the stronger frequency power. The second factor is the signal/background noise ratio; that is, the larger the signal/background noise ratio, the stronger the SIVV signal peak. Because of these factors, and in order to obtain the stronger SIVV signal, we should keep the background noise out of the ROI as much as possible. The more 'pure' the ridge and furrow signal, the stronger the signal. In summary, when determining the actual fingerprint ROI image, one must implement a trade-off between the size of the fingerprint region and the signal/noise ratio inside this region. Choose too small a region and the SIVV signal will be weak; choose too large a region such that it includes background noise and the SIVV signal will be buried.

2.5. Peak Location Constraint

Empirical data has shown frequency filtering to be an effective way to suppress background interferences associated with fingerprint evidence [6]. In the SIVV computation process, to extract the frequency information associated with an image, a 2D-Fast Fourier transform (FFT) can be computed. This computation will decompose a complicated spatial signal into individual frequencies, revealing both power spectrum and phase information. Under favorable circumstances, the frequencies associated with the friction ridge detail in the print will be separable from those frequencies associated with the interfering background features. Selective filtering of frequencies associated with fingerprint information may filter out the background interference and correctly locate the SIVV peak.

A fingerprint's SIVV frequency peak does not appear randomly in the frequency spectrum. The SIVV peak reflects the fingerprint's ridges and furrows' frequency. As we know, the physical distance between everyone's fingerprint ridges follows a certain statistical distribution in a certain range. If the image resolution of the image

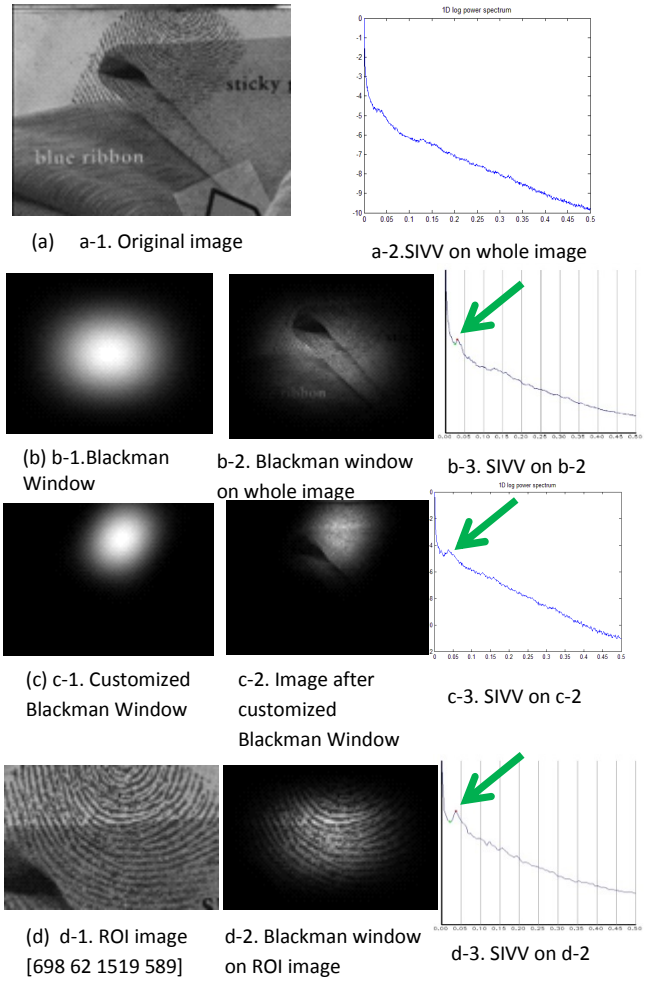

Figure 5: The comparison of SIVV curves using the whole image (051e), traditional Blackman window, customized Blackman window, and ROI.

sensor or scanner is given, the fingerprint ridges' pixel distances on the image in the spatial domain are fixed in a certain range. This range is directly related to the location of the SIVV fingerprint peak in the frequency domain. Figure 14 in [1] shows this concept. In the figure, the frequency locations of the SIVV peaks of the fingerprint image (1) mostly fall in a small range (between 0~0.15), which suggests that the fingerprint frequency of the SIVV peak can be constrained in a certain range in the frequency domain. Figure C-4, Figure C-5 and Figure C-6 in [1] also show the same concept, where most of the peak frequency locations of the SIVV feature in SD27 dataset also fall in a certain range, which shows a strong indication that we can constrain the SIVV peak location.

We ran a small experiment and verified that fingerprint ridges and the furrows' peak are directly related with the pixel distance between the strips (ridges) on the image, which means that in the latent fingerprint SIVV spectrum, under favorable circumstances, given the fingerprint

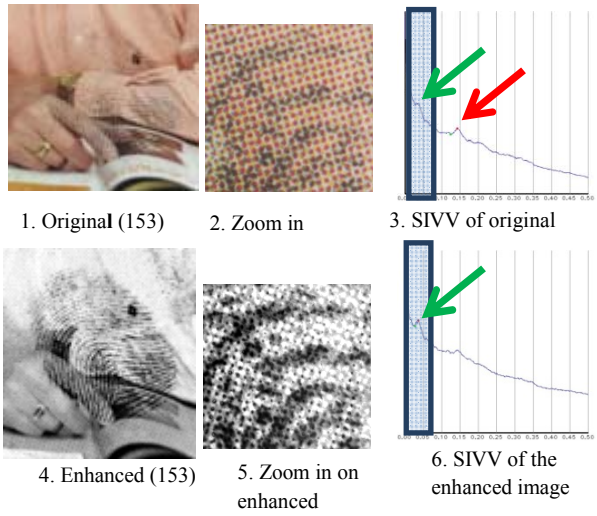

Figure 6: An example of SIVV peak location constraint.

ridges' distance range we can estimate the fingerprint frequency peak range. If there is a peak that is far away from this range, we can consider the peak generated by the background texture instead of the fingerprint (as shown by example 2 and 3 in Figure 3). In this way, the algorithm can selectively filter out the background interference to remove the fake peaks and correctly locate the SIVV peak.

Figure 6 shows an example where the original image SIVV spectrum is shown in the first row. The strongest peak is around 0.15 cycles/pixel (the red arrow in Figure 6-3). However, zooming in and looking closely at the details on the image in Figure 6-2, we can clearly see the grid texture in the background. The strong peak around 0.15 is actually not the fingerprint peak, it is the peak representing the frequency of the background texture. According to the fingerprint ridge distance in the image, the possible range for the fingerprint SIVV peak is indicated by the blue bar. The actual SIVV peak is the weak peak in the blue bar (the green arrow in Figure 6-3). The second row in Figure 6 gives the verification in another way. After the preprocessing process the

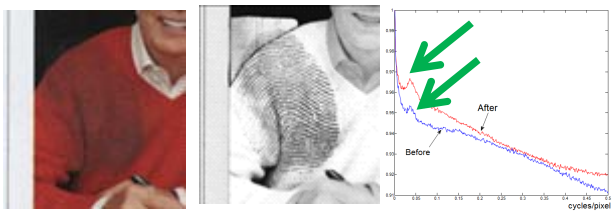

Figure 7: The comparison of SIVV curves of before and after images.

fingerprint signal is strengthened and the background noise is weakened. In this case, the SIVV peak located inside the predicted bar is the strongest peak while the background texture's peak is weakened and becomes smaller.

2.6. The comparison of before and after images on fingerprint preprocessing

In order to quantitatively measure the effectiveness of the preprocessing procedure, we proposed an algorithm, Fingerprint Quality Measurement (FQM) to compare the fingerprint image quality of before and after images. The SIVV curves of both before and after images are shown in Figure 7. It is obvious that the after image's SIVV peak (red curve) is stronger than the before image's SIVV peak (blue curve). Our objective is to propose an algorithm that can quantitatively compare the difference of the two peaks, so we can give a quantitative measurement of the effectiveness of the preprocessing process.

Figure 8 shows the proposed algorithm to compare the two images (before and after). Differing from the previous SIVV algorithm, we introduce several modifications to ensure the two SIVV curves are quantitatively comparable. Firstly, because the values of the direct current components (DC in Fourier spectrum) of the before and after images are different, the normalization step is removed from the new algorithm and replaced by the alignment step before the last comparison step. In

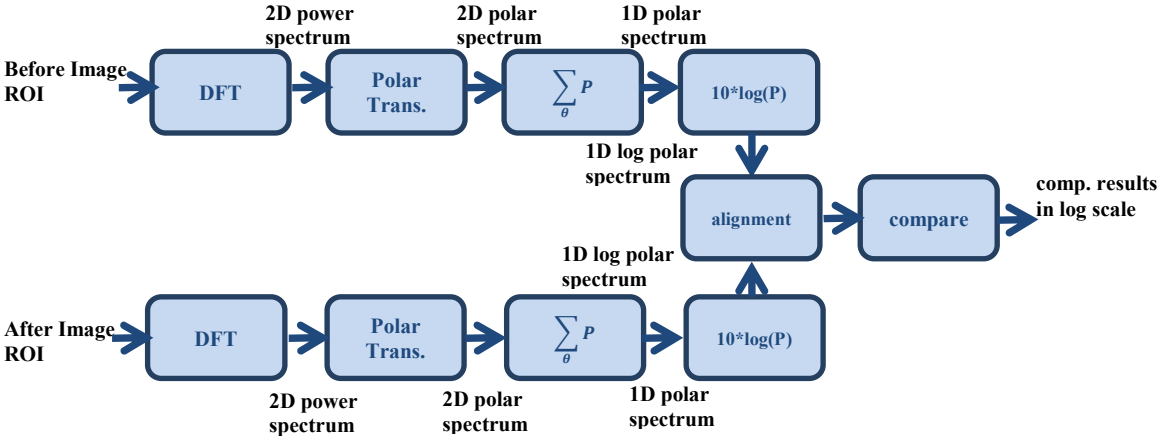

Figure 8: The algorithm to compare the before and after images using fingerprint quality measurement metric.

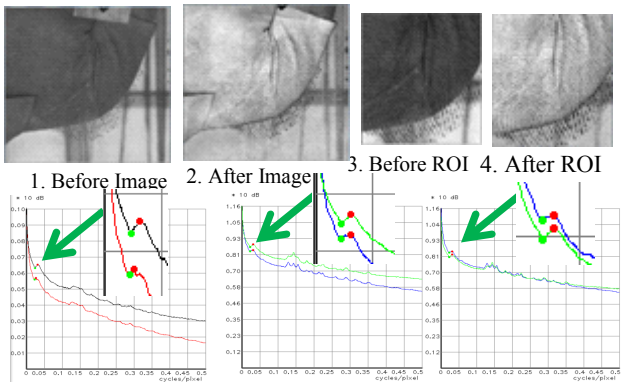

5. SIVV comparison (Before: red; After: black)

6. FQM comparison without alignment (Before: blue; After: green)

7. FQM comparison after alignment (Before: blue; After: green)

Figure 9: Evaluation of the enhancement procedure.

addition, in order to make the height of the peaks comparable, the algorithm performs the polar transformation before the logarithm calculation[5]. The logarithm expression is mainly for visualization. We aim to directly compare the differences of the fingerprint's ridge signal using power spectrum instead of logarithm power spectrum.

Figure 9 shows an example of the comparison. The proposed algorithm takes the before and after image pair as input (1 and 2 in Figure 9), then the user selects the fingerprint region ROI (3 and 4 in Figure 9). Figure 9-5 shows the comparison of SIVV on the before and after ROI. Figure 9-6 shows the proposed algorithm without the alignment and Figure 9-7 shows the proposed algorithm after the alignment.

Based on the proposed algorithm, we can further define the metrics which can quantitatively measure the success/effective of the preprocessing process. For example, Figure 10 shows the relative differences of the peak height ($\Delta h = h_{after} - h_{before}$), peak width ($\Delta w = w_{after} - w_{before}$), and peak area ($\Delta s = s_{after} - s_{before}$).

3. Experiment results

3.1. Latent fingerprint preprocessing dataset

We have a latent fingerprint preprocessing training dataset for our study. In the dataset, there are six types of latent fingerprint images: Bi-Chromatic mag powder developed prints, Bi-Chromatic powder developed prints, black ink pad on colored background, Ninhydrin developed prints, silver mag powder developed prints, and white powder developed prints. We use 39 forensic latent fingerprint image pairs in our experiment. Each pair has before image (RGB) and after image (grey). Each image

[5] The main difference can be expressed in the following mathematic way: $\log(P1 + P2)$ versus $\log P1 + \log P2 = \log(P1 * P2)$. In the comparison, we prefer $P1 + P2$ instead of $P1 * P2$.

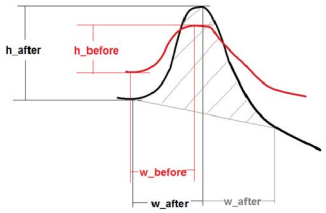

Figure 10: Proposed metrics to compare two latent fingerprint image qualities.

contains at least one latent fingerprint. The background for some images is very noisy. The fingerprint ridges and furrows are in low contrast and very blurry. Some images only contain a partial fingerprint image (less than ¼ fingerprint.).

3.2. ROI and ridge distance specification

Due to the poor quality of the latent fingerprints, automatic ROI extraction is a very challenging problem. In the experiment, we implemented an intuitive interactive graphical user interface to manually select ROI on the displayed input image. The user can click to adjust the top left corner of the ROI window and drag the cursor until the window is of the proper size. In the future, we may explore the use of a polygon to enhance the accuracy. In addition, we may also propose a semi-automatic ROI extraction method where, given the center of the fingerprint region and the radius of an ellipse which roughly covers the ROI, the algorithm automatically finds the maximum of the strongest SIVV signal peak and locates the accurate boundary of the ellipse.

We also created a user interface that allows the user to draw line segments (a user can draw the segment in the dense ridge area and the sparse ridge area respectively). The algorithm will automatically find the corresponding peak range in the frequency domain.

In the experiment, we used the following procedure: First, we manually select the region of interest. Then in the interested region, we choose the ridges with big gaps and draw several line segments from one ridge perpendicular

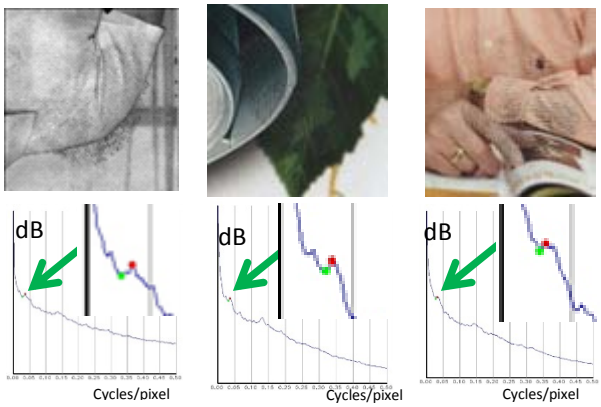

Figure 11: SIVV curves for some images using the proposed algorithms (ROI with peak location constraint).

to itself to another adjacent ridge, so the algorithm can measure the approximate distance between those two ridges. In the same way, we can choose the ridges with small gaps to input the approximate smallest distances between ridges. In the experiment, our maximum distance can be as large as twice the fingerprint ridge distance or as small as half of the fingerprint ridge distance. As long as the background noise's frequency is different than the fingerprint ridges' frequency, the algorithm works fine.

3.3. Comparisons using proposed procedures

We performed five experiments on our latent fingerprint enhancement dataset. If the correct SIVV peak is detected, we count it as true positive. We calculate the true positive rate (TPR): TPR = True Positive (TP) / (True Positive + False Negative). The five experiments were:

1. The SIVV package provided by NBIS [8], using the default option (all parameters are in default values). In this setting, the algorithm cuts the image first, then applies the Blackman filter, and calculates SIVV curve.
2. The SIVV package provided by NBIS, using the whole image option (all other parameters are in default values).
3. The SIVV package provided by NBIS, with a resized the input image (half of original width and height) (all other parameter are in default values). In this setting, the algorithm cuts the image first (different region from experiment 1), then applies the Blackman filter, and calculates SIVV curve.
4. A modified SIVV package with manual selection of ROI using a GUI interaction interface (all other parameters are in default values).
5. A modified SIVV package with manual selection of ROI, manually input the ridge distances by line segments using a GUI interaction interface (all other parameters are in default values).

The experiment results are shown in Table 1. It is clearly shown that the successful detection rates of the after images (the values in the second row) are much higher than the before images (the values in the first row), which indicates that the preprocessing process is extremely useful for some latent fingerprint images.

Table 1: The comparison of different implementations

TPR = TP/(TP+FN)	Original image Default option	Original image Whole option	Resize image Default option	Original image GUI ROI	GUI ROI Peak loc. Constraint
Before	36%	33%	62%	79%	85%
After	64%	72%	82%	87%	92%

Figure 11 shows SIVV curves for some images using the proposed algorithms (ROI with peak location constraint). It shows that the fingerprint signal (SIVV peak) is much stronger after the preprocessing process. In addition, it is also shown that the proposed approach performs well in the measurement of the latent fingerprint image's quality.

4. Discussions and Future Work

The research and study of the forensic latent fingerprint preprocessing using computational methods is still in an early stage. There is considerable further research and study required to provide a detailed scientific, systematic methodology to study latent fingerprint image preprocessing.

5. Acknowledgements

The authors thank Mathew Schwarz of Schwarz Forensics and David Witzke of Foray Technologies for valuable consultation on this work[6]. This research was supported by the 2012 NIST Forensic Measurement Challenges grant, "Metrics for Manipulation and Enhancement of Forensic Images".

References

[1] Libert, John M., John Grantham, and Shahram Orandi, a 1D spectral image validation/verification metric for fingerprints, NISTIR 7599, 2009.

[2] Robinson, Edward M. second edition, Crime scene photography. Chapter 10, Digital Imaging Technologies, contributions by David "Ski" Witzke, Academic Press, 2010.

[3] Indovina, Michael D., V. N. Dvornychenko, E. Tabasse, G. Quinn, P. Grother, M. Garris, and S. Meagher. ELFT Phase II: An Evaluation of Automated Latent Fingerprint Identification Technologies. US Department of Commerce, National Institute of Standards and Technology, 2009.

[4] Yen, Robert, and Joseph Guzman. "Fingerprint image quality measurement algorithm." Journal of Forensic Identification 57, no. 2 (2007): 274.

[5] Fierrez-Aguilar, Julian, Yi Chen, Javier Ortega-Garcia, and Anil Jain. "Incorporating image quality in multi-algorithm fingerprint verification." Advances in Biometrics (2005): 213-220.

[6] Yoon, Soweon, Jianjiang Feng, and Anil K. Jain. "On latent fingerprint enhancement." *SPIE Defense, Security, and Sensing*. International Society for Optics and Photonics, 2010.

[7] Garris, Michael D., and R. Michael McCabe. "NIST special database 27: Fingerprint minutiae from latent and matching tenprint images." NIST, Gaithersburg, MD. [CD-ROM] NIST Tech. Rep. NISTIR 6534.

[8] NIST Biometric Image Software, http://www.nist.gov/itl/iad/ig/nbis.cfm, NIST USA.

[6] Disclaimer: Any mention of commercial products or reference to commercial organizations is for information only; it does not imply recommendation or endorsement by NIST nor does it imply that the products mentioned are necessarily the best available for the purpose.